

# NASA

*100-217  
3-11-59*

## MEMORANDUM

WATER-LANDING CHARACTERISTICS OF A REENTRY CAPSULE

By John R. McGehee, Melvin E. Hathaway,  
and Victor L. Vaughan, Jr.

Langley Research Center  
Langley Field, Va.

**NATIONAL AERONAUTICS AND  
SPACE ADMINISTRATION**

WASHINGTON

June 1959



NATIONAL AERONAUTICS AND SPACE ADMINISTRATION

---

MEMORANDUM 5-23-59L

---

WATER-LANDING CHARACTERISTICS OF A REENTRY CAPSULE

By John R. McGehee, Melvin E. Hathaway,  
and Victor L. Vaughan, Jr.

SUMMARY

Experimental and theoretical investigations have been made to determine the water-landing characteristics of a conical-shaped reentry capsule having a segment of a sphere as the bottom. For the experimental portion of the investigation, a 1/12-scale model capsule and a full-scale capsule were tested for nominal flight paths of  $65^\circ$  and  $90^\circ$  (vertical), a range of contact attitudes from  $-30^\circ$  to  $30^\circ$ , and a full-scale vertical velocity of 30 feet per second at contact. Accelerations were measured by accelerometers installed at the centers of gravity of the model and full-scale capsules. For the model test the accelerations were measured along the X-axis (roll) and Z-axis (yaw) and for the full-scale test they were measured along the X-axis (roll), Y-axis (pitch), and Z-axis (yaw). Motions and displacements of the capsules that occurred after contact were determined from high-speed motion pictures. The theoretical investigation was conducted to determine the accelerations that might occur along the X-axis when the capsule contacted the water from a  $90^\circ$  flight path at a  $0^\circ$  attitude. Assuming a rigid body, computations were made from equations obtained by utilizing the principle of the conservation of momentum. The agreement among data obtained from the model test, the full-scale test, and the theory was very good. The accelerations along the X-axis, for a vertical flight path and  $0^\circ$  attitude, were in the order of  $40g$ . For a  $65^\circ$  flight path and  $0^\circ$  attitude, the accelerations along the X-axis were in the order of  $50g$ . Changes in contact attitude, in either the positive or negative direction from  $0^\circ$  attitude, considerably reduced the magnitude of the accelerations measured along the X-axis. Accelerations measured along the Y- and Z-axes were relatively small at all test conditions.

INTRODUCTION

One of the proposed methods for manned space flight employs a conical-shaped capsule as the vehicle. The base of the capsule, designed to serve as a heat shield upon reentry, is a segment of a sphere. After reentry a parachute would be used for the letdown to a water landing. Based upon this method of letdown and landing, experimental and theoretical

investigations have been conducted to determine the water-landing characteristics of this type of capsule.

To simulate some of the possible flight paths and contact attitudes that might occur with a parachute letdown, the experimental investigations were conducted for nominal flight paths of  $65^\circ$  and  $90^\circ$ , a range of contact attitudes from  $-30^\circ$  to  $30^\circ$ , and a full-scale vertical velocity of 30 feet per second at contact. These flight paths were chosen to represent parachute letdowns that might occur with surface winds of 14 and 0 feet per second. The various contact attitudes were chosen to represent a range of possible contact attitudes that might occur if, upon landing, the capsule were swinging beneath the parachute. For the gross weight under consideration the vertical contact velocity of 30 feet per second could be obtained with a conventional parachute.

The theoretical investigation was conducted for a flight path of  $90^\circ$  and a contact attitude of  $0^\circ$ . The equations, from which the computations were made, were based upon the principle of the conservation of momentum during the water impact.

#### SYMBOLS

$g$	acceleration due to gravity, 32.2 ft/sec <sup>2</sup>
$h$	vertical position of center of gravity from free-water surface, ft
$\Delta h$	displacement of center of gravity, ft
$I$	moment of inertia, slug-ft <sup>2</sup>
$m_w$	virtual mass of water, lb
$R$	radius of spherical bottom, ft
$t$	time from instant of contact, sec
$\Delta t$	change in time, sec
$V_0$	initial vertical velocity, ft/sec
$V_t$	vertical velocity at time $t$ , ft/sec
$\Delta V$	change in vertical velocity, ft/sec

W	weight of capsule, lb
$\rho$	mass density of water (1.94 slug/ft <sup>3</sup> for model test; 1.99 slug/ft <sup>3</sup> for full-scale test)

## APPARATUS AND PROCEDURE

A drawing of the capsule configuration is shown in figure 1. The orientation of axes, the flight path, and the attitude used in the investigation are shown in figure 2. Pertinent dimensions and moments of inertia for the model and the full-scale capsule as measured are listed in table I.

### Model Capsule

The 1/12-scale dynamic model was constructed of fiber glass and plastic and the construction was as rigid as possible to eliminate secondary vibrations. Two strain-gage-type accelerometers were located at the center of gravity and rigidly mounted to the bottom of the model. The accelerometers were capable of recording accelerations of 200g and 25g along the X- and Z-axes, respectively. The signals from the accelerometers were transmitted through cables to amplifying and recording equipment on shore. The natural frequency of the 200g accelerometer was about 900 cycles per second and that of the 25g accelerometer was about 350 cycles per second. The accelerometers were damped to 65 percent of critical damping. The response of the recording equipment was flat to about 2,200 cycles per second.

The model tests for the 90° flight path were made by a free-fall method where the model was dropped from the required height to obtain a full-scale speed of 30 feet per second at water contact. The model tests for the 65° flight path were conducted using a catapult type of test apparatus as shown in figure 3. The catapult consisted of a steel staff which followed the flight path by moving through a rigidly mounted roller cage. A yoke, which held the model by the use of pins inserted into sleeves at the edge of the model base, was mounted at the bottom of the staff. The pins were under spring tension and would retract at the end of the catapult stroke to free the model. The model was held at the desired attitude by a sting which was fixed to the staff and inserted into the top of the model. The staff, under the influence of gravity, would run through the roller cage and various speeds were obtained by varying the stroke. The velocity of the catapult was measured by recording the time for the staff to travel the last 2 inches of the catapult stroke. An electronic counter recorded the time. The counter was capable of recording time to 1/100,000 of a second. The

catapult velocity was combined with the velocity computed for the free-fall height, which was the height between the model release point and the water surface, to obtain the actual contact velocity. The contact attitude and motions of the capsule after contact were recorded by a high-speed motion-picture camera. The tests were conducted in calm water in Langley tank No. 2 which has a water depth of 6 feet.

### Full-Scale Capsule

The body of the full-scale capsule was constructed of 0.25-inch magnesium alloy and the base was formed from 1.00-inch magnesium alloy. In order to obtain the desired weight and center-of-gravity location, it was necessary to install a pedestal on the bottom of the capsule for attaching weights. Accelerometers were rigidly attached to the pedestal at the capsule center of gravity. These accelerometers were positioned to measure accelerations along the X-, Y-, and Z-axes and were capable of measuring 100g, 20g, and 50g, respectively. The signals from the accelerometers were transmitted through cables to amplifying and recording equipment on shore. The natural frequency of the 100g accelerometer was about 640 cycles per second, that of the 50g accelerometer was about 370 cycles per second, and that of the 20g accelerometer was about 160 cycles per second. The accelerometers were damped to 65 percent of critical damping. The response of the recording equipment for the 100g accelerometer was flat to 600 cycles per second and that for the 20g and 50g accelerometers was flat to 190 cycles per second. Velocities, contact attitudes, and flight paths were recorded by high-speed motion-picture cameras.

For the full-scale test a procedure utilizing gravitational acceleration for obtaining desired velocities and the principle of the pendulum for obtaining flight paths was developed. A 20-ton crane with a 75-foot boom was used to drop the capsule in the full-scale test. A photograph of the test setup for a 65° flight path and a nominal 30° contact attitude is shown in figure 4. For the 90° flight-path drops, the capsule was suspended at the desired contact attitude and dropped vertically from the height necessary to establish, under the influence of gravity, a full-scale vertical contact velocity of 30 feet per second. For the 65° flight-path drops the lift cable was used to suspend the model at the various contact attitudes and the drag line was used to pull the capsule through the desired pullback angle. All fittings on the capsule were mounted so that the forces applied by the lift and pullback cables would act through the capsule center of gravity and thus minimize any tendency for the capsule to oscillate when released. Electrically operated aircraft bomb shackles were attached to the lift and pullback cables for releasing the capsule. The bomb shackles operated with a minimum of influence upon the motions of the capsule. An electrical triggering circuit was developed for controlling the time interval between operation of pullback and lift releases.

A 1/12-scale-model test was performed, using the procedure outlined for the full-scale test, to determine the reliability of the proposed procedure. The results obtained from this test indicated that the procedure would satisfactorily accomplish the desired results.

The full-scale test was conducted at Langley Field, Va. The test was made in a depression approximately 11 feet deep and 50 feet in diameter (approximately 20 feet offshore) and was performed in relatively calm weather to avoid the influence of large waves.

### Computations

The classical impact theory of Von Kármán (as stated in ref. 1) for vertical impact of a wedge at  $0^\circ$  trim is based on the concept that during the course of an impact the momentum lost by the impacting body can be considered to be transferred to some finite mass of water in contact with the body which has a downward velocity equal to that of the body. Since the entire initial momentum of the body is thus assumed to be distributed between the body and the virtual mass of water, the momentum of the body and the virtual mass is constant throughout the impact, and the motions of the body subsequent to the instant of initial contact can be determined from the basic relationship

$$\left(\frac{W}{g}\right)V_0 = \left(\frac{W}{g} + m_w\right)V_t$$

if the variation of the virtual mass  $m_w$  is specified.

Von Kármán proposed that the virtual mass be taken equal to the mass of a semicylinder of water having a diameter equal to the instantaneous width of the body in the plane of the undisturbed water surface. In applying this theory to the impact of three-dimensional bodies, it is assumed that the virtual mass can be taken equal to three-quarters of the mass of a hemisphere of water having a diameter equal to the instantaneous width of the body in the plane of the undisturbed water surface. The arbitrary factor of three-quarters is an approximate correction indicated to be desirable by data from the impact of wedges (ref. 2). If a rigid body is assumed the equation for the velocity at any given time can be written as

$$V_t = \frac{WV_0}{W + \left(\frac{3}{4}\right)\frac{2\pi}{3} \rho g R^3 \left[ \sin^3 \arccos \left(1 - \frac{h}{R}\right) \right]}$$

and the acceleration equals the change in velocity over the change in time. Buoyancy and gravity are not included in the calculations since they become important only in later stages of severe impacts. The concept is not valid when there is an appreciable component of velocity parallel to the water surface. In such a condition the motion of the body along the surface causes a loss of momentum to a quantity of water detached from the body, thus violating the assumption of momentum conservation between the body and its attached virtual mass. No computations were therefore made for the inclined flight path.

## RESULTS AND DISCUSSION

A short motion-picture film supplement illustrating the effects discussed in this paper is available on loan. A request card form and a description of the film will be found at the end of this paper, on the page immediately preceding the abstract and index pages.

### Presentation of Results

Model capsule.- The experimental data for the model capsule are presented in table II. Typical time histories of the accelerations along the X-axis are shown in figure 5. A photograph showing the model after contact at a  $-33^\circ$  attitude from a  $65^\circ$  flight path is shown in figure 6. Peak accelerations along the X-axis, from data such as those presented in figure 5, are shown plotted in figure 7 as a function of contact attitude with flight-path angle as a parameter. The peak accelerations experienced by this type of capsule were of the order of 40g for a contact attitude of  $0^\circ$  and a vertical flight path. For a contact attitude of  $0^\circ$  and a flight path of  $65^\circ$ , the peak accelerations were in the order of 50g. Within the accuracy of the tests this increase may be attributed to the increased velocity along the  $65^\circ$  flight path as compared with the velocity along the vertical flight path. For a vertical flight path, a change in contact attitude from  $0^\circ$  to  $33^\circ$  resulted in a reduction in the peak acceleration from approximately 40g to approximately 8g. This reduction in peak acceleration may be attributed to the wedge shape of the impact surface of the capsule at the  $33^\circ$  attitude as compared with the blunt impact surface for the  $0^\circ$  attitude. Impact on the wedge-shaped surface resulted in a lower rate of increase of the virtual mass which resulted in lower accelerations and greater penetrations. In order to illustrate this effect further, the contact attitudes of  $0^\circ$ ,  $19^\circ$ , and  $-34^\circ$ , for the  $65^\circ$  flight path resulted in peak accelerations of 53g, 17g, and 6g, respectively. In general, the time to reach peak acceleration increased as the magnitude of the peak accelerations decreased. (See fig. 5.) Accelerations measured along the Z-axis were relatively small at all test conditions. (See table II.)



Typical pitch angles and vertical displacements of the model after contact are shown in figure 8. The drop for a  $0^\circ$  contact attitude from a vertical flight path had very small variations in pitch angles. For the drop made for a  $27^\circ$  contact attitude from a  $68^\circ$  flight path, the model pitched in a negative direction after contact and then righted itself. For the remaining drops shown in figure 8, the model pitched in a positive direction after contact and, with the impact of a following wave, the model pitched in a negative direction and then recovered to an upright position. The vertical displacements of the center of gravity were similar for the various contact attitudes and flight paths.

Full-scale capsule.- The experimental data for the full-scale capsule are presented in table III and typical acceleration-time histories determined for the X-axis are shown in figure 9. The remarks previously made concerning the accelerations for the model test are applicable to the full-scale test. The accelerations are similar to those determined from the model test for approximately the same flight paths and contact attitudes. The photograph in figure 10 shows the capsule after contact at an  $18^\circ$  attitude from a  $65^\circ$  flight path.

Typical pitch angles and vertical displacements of the full-scale capsule after contact are shown in figure 11. In general, the variations in pitch angles and vertical displacements of the full-scale capsule are similar to those determined from the model test.

#### Comparison of Data

Peak accelerations.- Comparisons of peak accelerations along the X-axis obtained from the model test, full-scale test, and theoretical investigation are shown in figure 12 as a function of contact attitude with flight-path angle as a parameter. The curves represent fairings of the data obtained from the model test. Superimposed upon these curves are the data obtained from the full-scale test and the theoretical investigation (data calculated from the theory are given in table IV). As shown in this figure the agreement is excellent. The magnitude of the peak accelerations was considerably reduced by changes in contact attitude in either the positive or negative direction from  $0^\circ$  attitude.

Acceleration-time histories.- Acceleration-time histories determined from the model test, full-scale test, and theoretical investigation are compared in figure 13 for a flight path of  $90^\circ$  and a contact attitude of  $0^\circ$ . As can be seen in this figure, the agreement among the acceleration-time histories was good.

Pitch angles and vertical displacements.- Pitch angles and vertical displacements of the model and full-scale capsule are compared in figure 14

for a nominal flight path of  $65^\circ$  and a nominal contact attitude of  $-23^\circ$ . These comparisons are made for drops of the model with attached instrument cable, the model without instrument cable, and the full-scale capsule with instrument cable. The vertical displacements of the three drops were approximately the same. There was good agreement between the pitch angles of all of the drops for 2 seconds after contact, but after 2 seconds the pitch angles of the model with the instrument cable attached deviated, probably because of the restraining influence of the instrument cable. The pitch angles for the full-scale capsule and the model without instrument cable are approximately the same. The deviation shown for that portion of the drop in which the capsule was returning to an upright position may have been caused by the effect of the surface tension of the water on the model as compared with the negligible effect of the surface tension on the full-scale capsule. This deviation may also have been partly caused by the effect of the instrument cable on the full-scale capsule.

#### CONCLUDING REMARKS

Experimental and theoretical investigations have been made to determine the water-landing characteristics of a conical-shaped reentry capsule having a segment of a sphere as the bottom. The peak accelerations along the X-axis experienced by this type of capsule were in the order of  $40g$  for a contact attitude of  $0^\circ$  and a vertical flight path. For a contact attitude of  $0^\circ$  and a flight path of  $65^\circ$ , the peak accelerations were in the order of  $50g$ . Changes in contact attitude in either the positive or negative direction from  $0^\circ$  attitude resulted in a considerable reduction in the peak accelerations. Accelerations measured along the Y- and Z-axes were relatively small at all test conditions.

Excellent agreement was obtained among the peak accelerations of the model, full-scale, and rigid-body theoretical investigations.

Langley Research Center,  
National Aeronautics and Space Administration,  
Langley Field, Va., March 3, 1959.

## REFERENCES

1. Milwitzky, Benjamin: Generalized Theory for Seaplane Impact. NACA Rep. 1103, 1952.
2. Bisplinghoff, R. L., and Doherty, C. S.: A Two-Dimensional Study of the Impact of Wedges on a Water Surface. Contract No. NOa(s)-9921, Dept. Aero. Eng., M.I.T., Mar. 20, 1950.

TABLE I

## PERTINENT DIMENSIONS

	Model capsule (1/12 scale), measured values	Full-scale capsule	
		Measured values	Converted to model scale
Weight . . . . .	1.32 lb	2,150 lb	1.24 lb
Height (overall) . . . .	10.50 in.	10.5 ft	10.50 in.
Radius of spherical bottom . . . .	10.50 in.	10.5 ft	10.50 in.
Base diameter . . . . .	7.00 in.	7.0 ft	7.00 in.
Center-of-gravity location (height from bottom) . . . . .	2.10 in.	2.33 ft	2.33 in.
$I_{pitch}$ . . . . .	0.00181 slug-ft <sup>2</sup>	540 slug-ft <sup>2</sup>	0.00226 slug-ft <sup>2</sup>
$I_{yaw}$ . . . . .	0.00176 slug-ft <sup>2</sup>	540 slug-ft <sup>2</sup>	0.00226 slug-ft <sup>2</sup>

TABLE II

## MODEL DATA

[Converted to full scale]

Attitude at contact, deg	Flight path, deg	Vertical velocity at contact, fps	Horizontal velocity at contact, fps	Accelerations		Time to peak	
				Along X-axis, g	Along Z-axis, g	Along X-axis, sec	Along Z-axis, sec
0	90	29.5	0	42.5	0	0.003	-----
0	90	29.7	0	42.5	0	.003	-----
0	90	29.6	0	41.6	0	.003	-----
1	90	30.2	0	42.5	0	.003	-----
0	90	29.6	0	40.7	0	.003	-----
0	90	29.5	0	41.6	0	.003	-----
33	90	28.9	0	7.4	1.5	.019	0.019
33	90	28.9	0	8.0	1.5	.019	.019
33	90	29.0	0	7.4	1.5	.019	.019
0	65	29.9	13.6	53.0	0	.003	-----
0	65	29.7	13.5	53.0	0	.003	-----
0	65	29.7	13.5	53.0	0	.003	-----
-6	72	30.0	9.8	52.6	0	.003	-----
-4	69	28.8	11.0	54.8	0	.003	-----
6	70	30.2	11.0	47.0	0	.003	-----
7.5	71	29.3	10.4	33.5	0	.003	-----
5	68	28.6	11.5	41.6	0	.003	-----
26	68	31.6	12.3	11.5	-2.0	.014	.003
19	68	28.6	11.5	17.2	-3.8	.005	.003
19	68	28.0	11.3	18.1	-3.3	.005	.005
-21	70	28.1	9.1	14.5	3.9	.005	.005
-38	68	29.5	12.1	5.4	3.9	.017	.017
-36	66	32.3	14.2	8.2	3.4	.018	.008
-34	69	29.3	11.1	5.8	2.6	.014	.016
-35	70	28.5	10.5	4.5	2.6	.019	.019
-35	67	29.9	12.6	5.7	3.7	.017	.024

TABLE III

## FULL-SCALE DATA

Attitude at contact, deg	Flight path, deg	Vertical velocity at contact, fps	Horizontal velocity at contact, fps	Accelerations			Time to peak			Average angular velocity during free fall, rad/sec
				Along X-axis, g	Along Y-axis, g	Along Z-axis, g	Along X-axis, sec	Along Y-axis, sec	Along Z-axis, sec	
0	90	30.0	0	40.6	-1.4	0	0.002	0.002	-----	0
0	90	30.2	0	43.5	0	0	.003	-----	-----	0
0	90	30.9	0	41.2	0	0	.002	-----	-----	0
1	65	30.7	16.4	49.0	0	0	.002	-----	-----	-----
1	61	30.0	16.4	51.0	1.1	0	.002	.0015	-----	.45
-2	66	31.0	14.7	49.0	1.2	0	.002	.0015	-----	.52
-3	66	31.7	13.7	49.0	1.2	0	.0015	.0010	-----	.38
18	65	30.7	13.5	21.0	0	0	.0060	-----	-----	.20
17	65	30.1	14.2	22.5	0	0	.0050	-----	-----	.15
18	65	28.5	13.7	21.0	0	0	.0055	-----	-----	.15
-23.5	65	32.2	14.9	10.0	0	3.7	.0100	-----	0.0120	.35
-24.7	65	30.8	13.5	10.0	0	3.7	.0090	-----	.0130	.35
26	90	29.6	0	9.0	0	0	.0100	-----	-----	0
26	90	29.1	0	10.0	0	0	.0100	-----	-----	.04
26.5	90	29.4	0	9.0	0	0	.0090	-----	-----	.04

TABLE IV

THEORETICAL DATA

(1)	(2)	(3)	(4)	(5)	(6)	(7)	(8)	(9)	(10)	(11)	(12)	(13)
t, sec	$\Delta t$ , sec	$\Delta h = \frac{(11)}{(2)} \times (2)$ (a)	$h = \sum (3)$	$\frac{h}{R} = \frac{(4)}{10.5}$	$1 - (5)$	$\sin \cos^{-1} \left( 1 - \frac{h}{R} \right)$	$(7)^3$	$115,114 \times (8)$	$(9) + 2,150 V_t$	$V_t = \frac{64,500}{(10)}$	$\Delta V$	$\frac{(12)}{(2)g}$
0	0.001	0.03000	0.03000	0.00286	0.99714	0.07556	0.00043	49.50	2,199.50	30.00	0.68	0
.001	.001	.02932	.05932	.00565	.99435	.10616	.00120	138.14	2,288.14	28.19	1.13	21.1
.002	.001	.02819	.08751	.00833	.99167	.12880	.00214	246.34	2,396.34	26.92	1.27	35.1
.003	.001	.02692	.11443	.01090	.98910	.14723	.00319	367.21	2,517.21	25.62	1.50	39.4
.004	.001	.02562	.14005	.01334	.98666	.16281	.00432	497.29	2,647.29	24.36	1.26	40.4
.005	.001	.02436	.16441	.01566	.98434	.17629	.00548	650.82	2,780.82	23.19	1.17	39.1
.006	.001	.02319	.18760	.01787	.98213	.18819	.00667	767.81	2,917.81	22.11	1.08	36.3
.007	.001	.02211	.20971	.01997	.98003	.19885	.00786	904.80	3,054.80	21.11	1.00	33.5
.008	.001	.02111	.23082	.02198	.97802	.20853	.00907	1,044.08	3,194.08	20.19	.92	31.1
.009	.001	.02019	.25101	.02391	.97609	.21738	.01027	1,182.22	3,331.22	19.36	.83	28.6
.010	.001	.03872	.28973	.02759	.97441	.23329	.01270	1,461.95	3,611.95	17.86	1.50	23.3
.012	.002	.03572	.32545	.03100	.96900	.24707	.01508	1,735.92	3,885.92	16.60	1.26	19.6
.014	.002	.03320	.35865	.03416	.96584	.25914	.01740	2,002.98	4,152.98	15.53	1.07	16.6
.016	.002	.03106	.38971	.03712	.96288	.26993	.01967	2,264.29	4,414.29	14.61	.92	14.3
.018	.002	.02922	.41893	.03990	.96010	.27966	.02187	2,517.54	4,667.54	13.82	.79	12.3
.020	.002	.02922	.44803	.04648	.95552	.30132	.02736	3,149.52	5,299.52	12.17	1.65	10.3
.025	.005	.06910										

<sup>a</sup>Use column (11) for  $t = t - \Delta t$ .

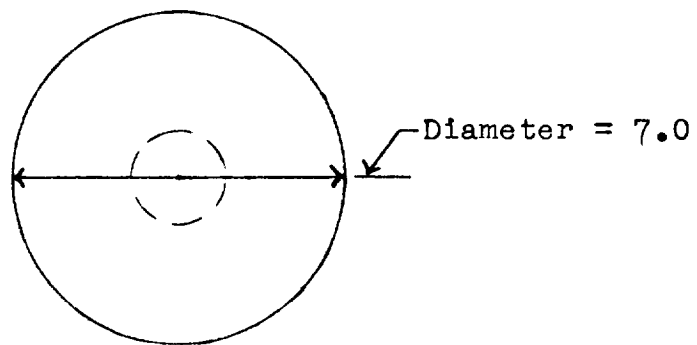
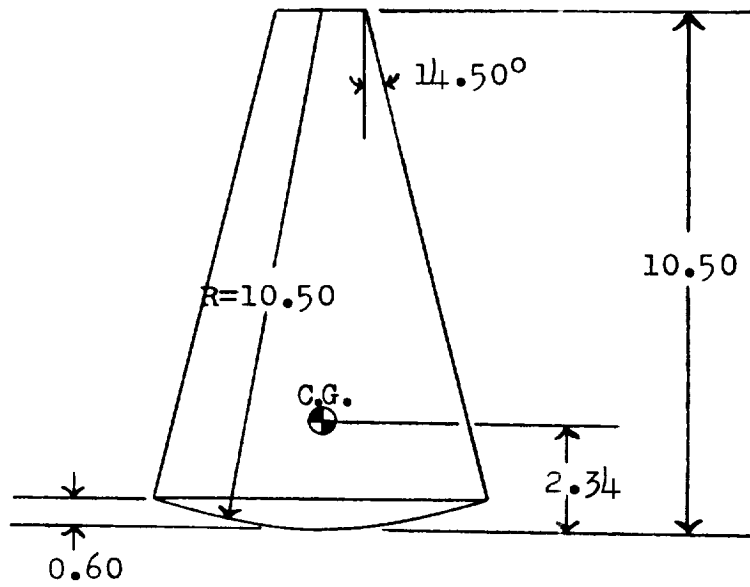


Figure 1.- Capsule configuration. (All dimensions are in feet, full scale.)



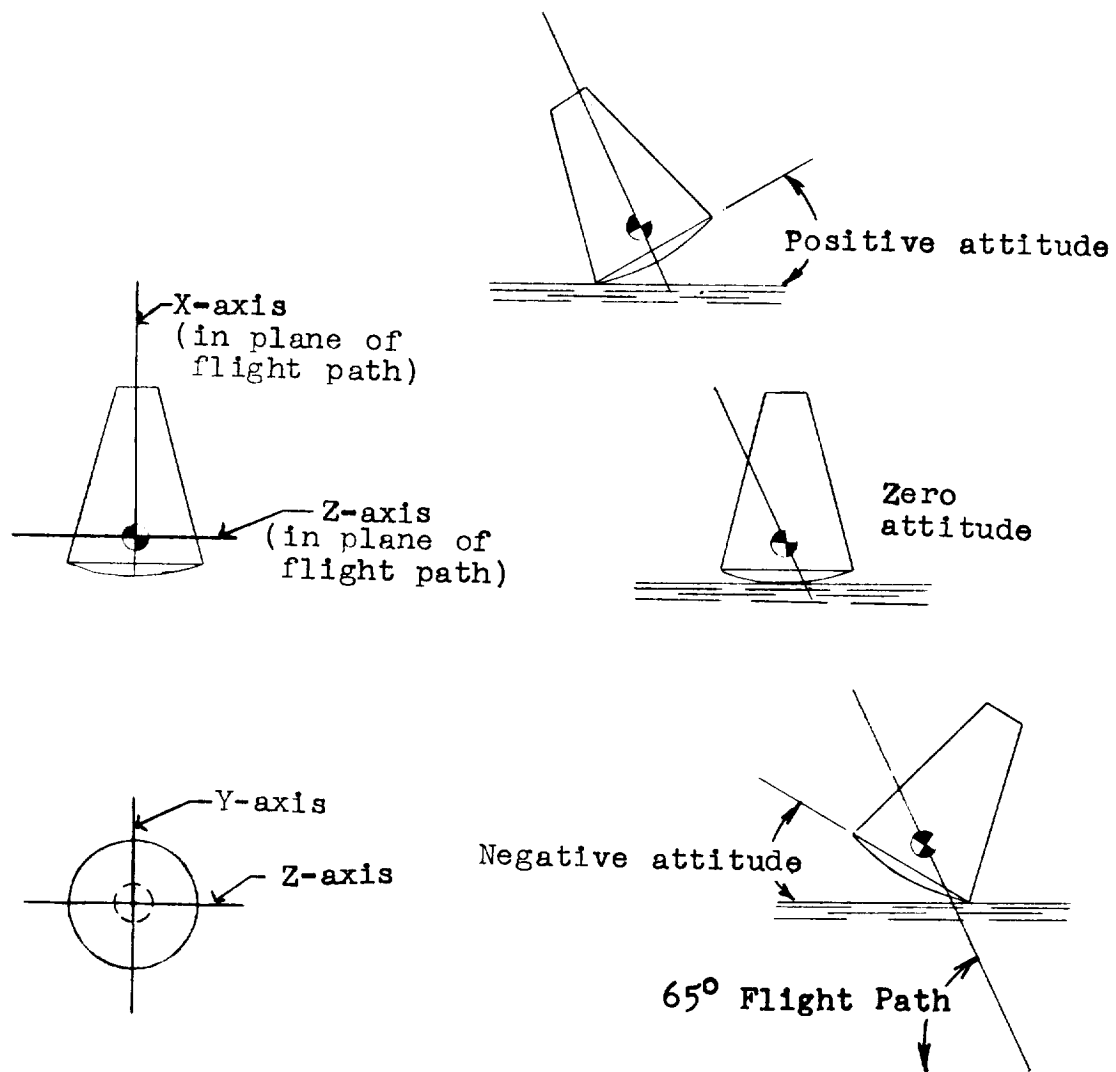


Figure 2.- Sketches identifying axes, flight paths, and impact attitudes.

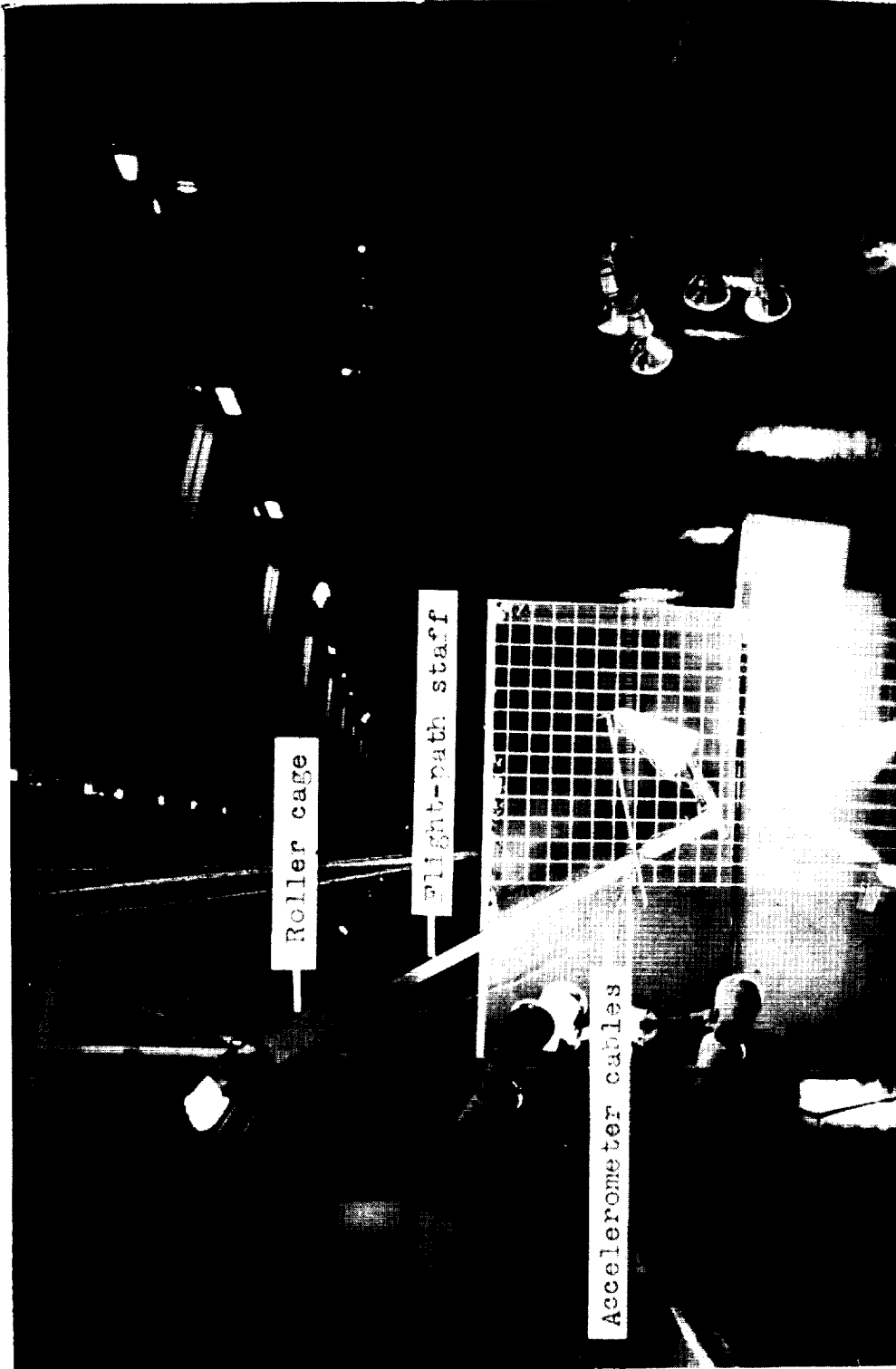
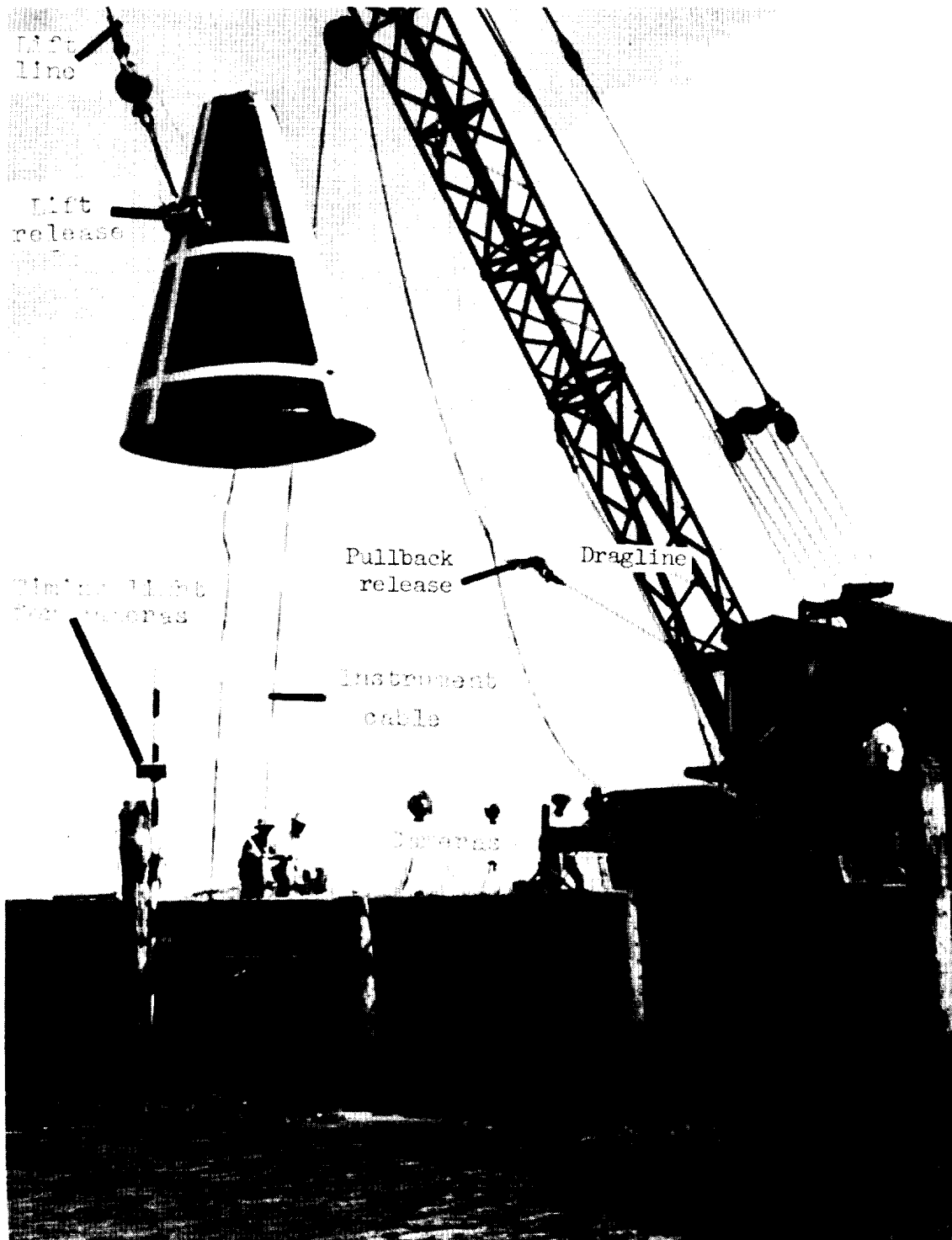


Figure 3.- Model test setup. I-58-2860.1



L-58-3338.1  
 Figure 4.- Full-scale test setup for nominal  $65^\circ$  flight path and nominal  $30^\circ$  attitude.

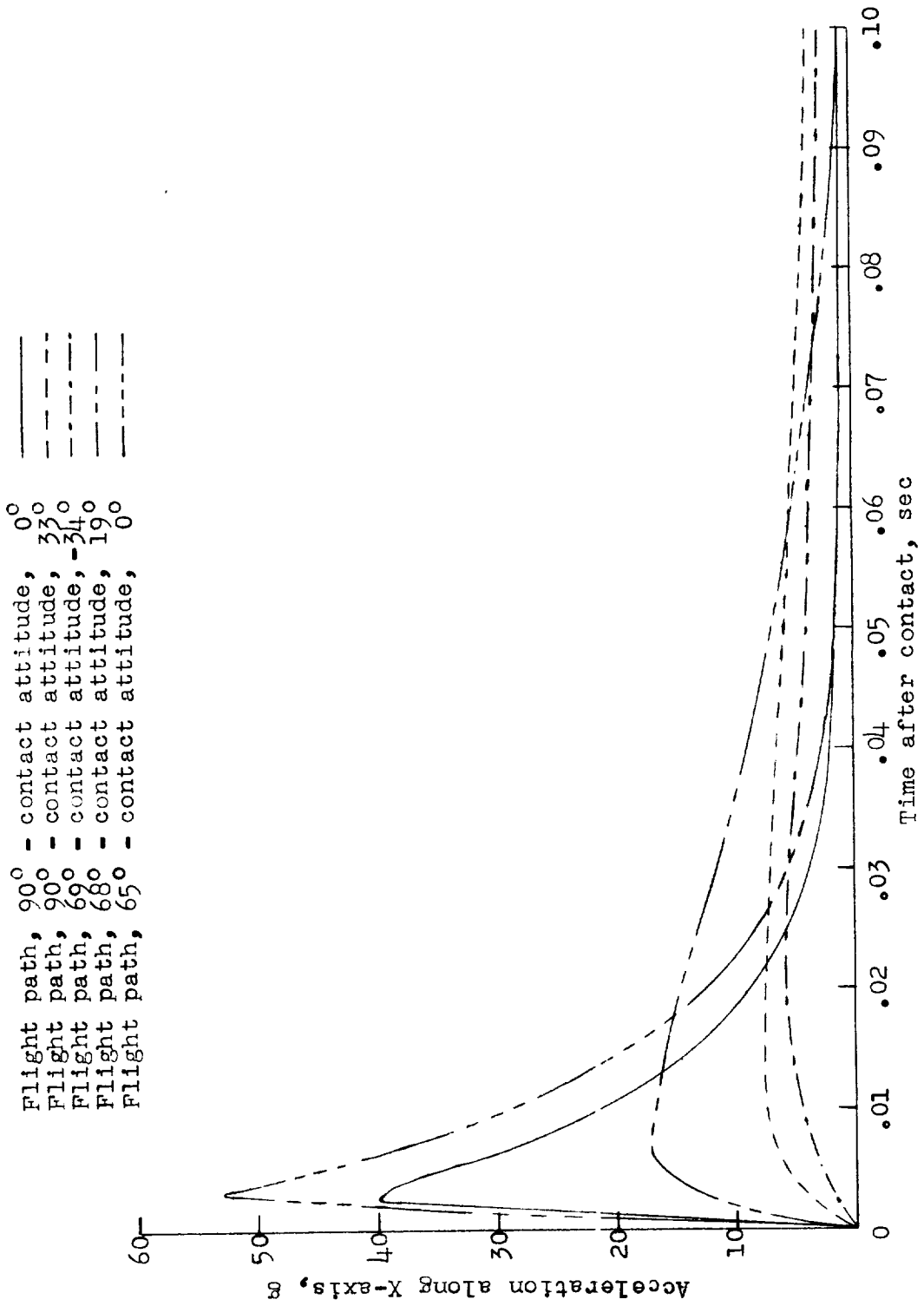


Figure 5.- Typical acceleration-time histories determined from model test. (Values converted to full scale.)

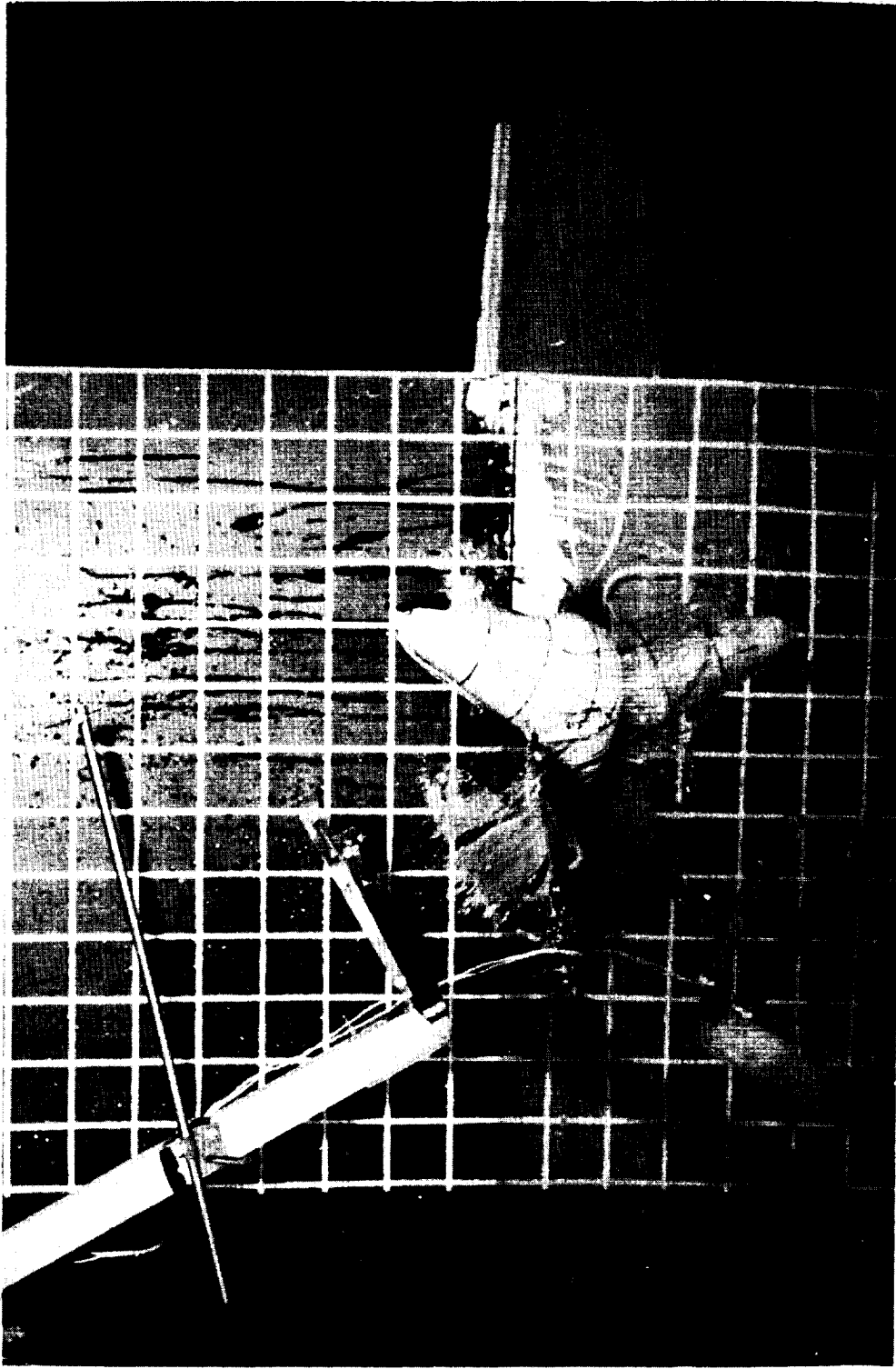


Figure 6.- Model capsule after contact at a  $-33^{\circ}$  attitude from a  $65^{\circ}$  flight path. I-58-2863

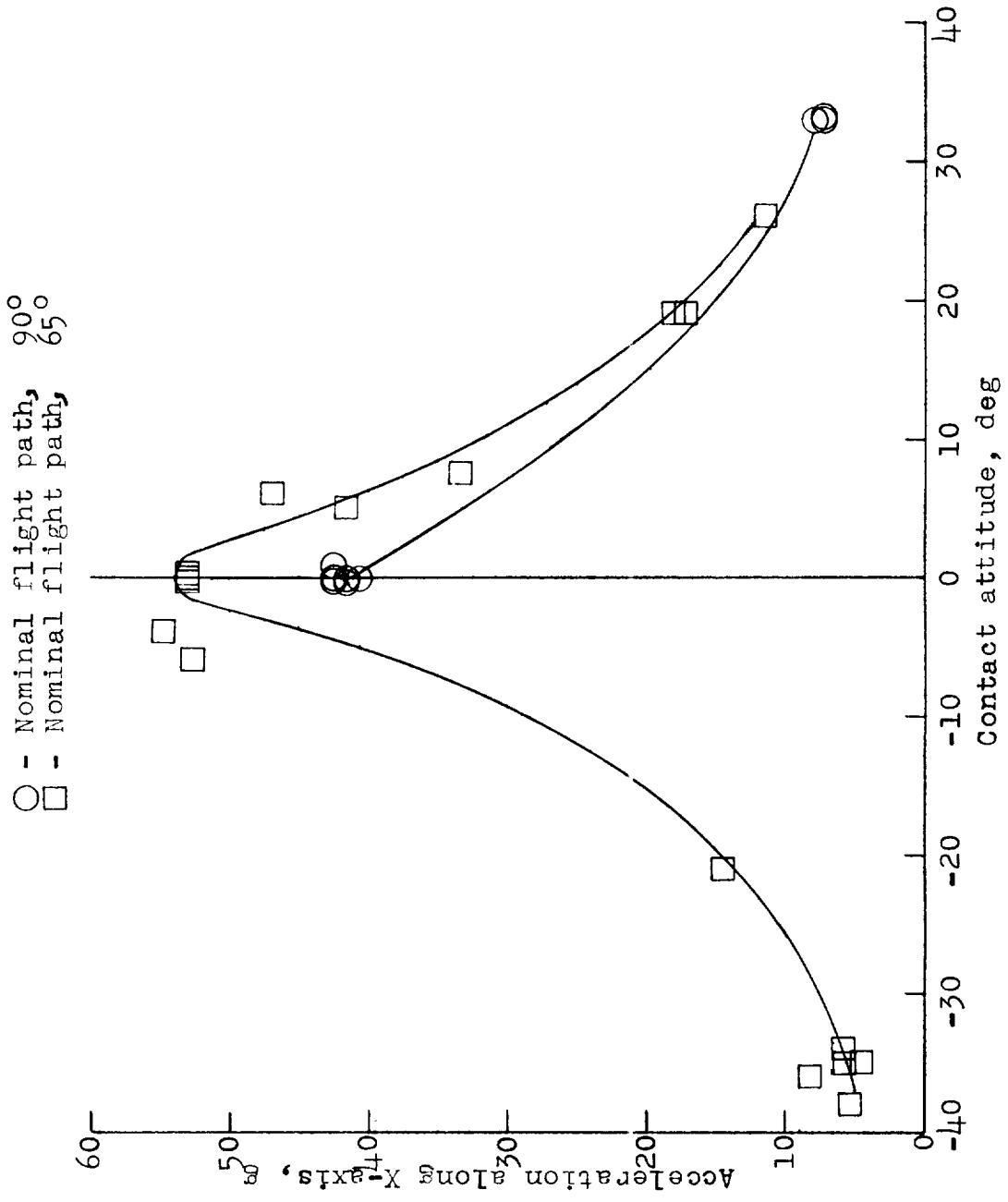


Figure 7.- Maximum accelerations along X-axis obtained from model test.

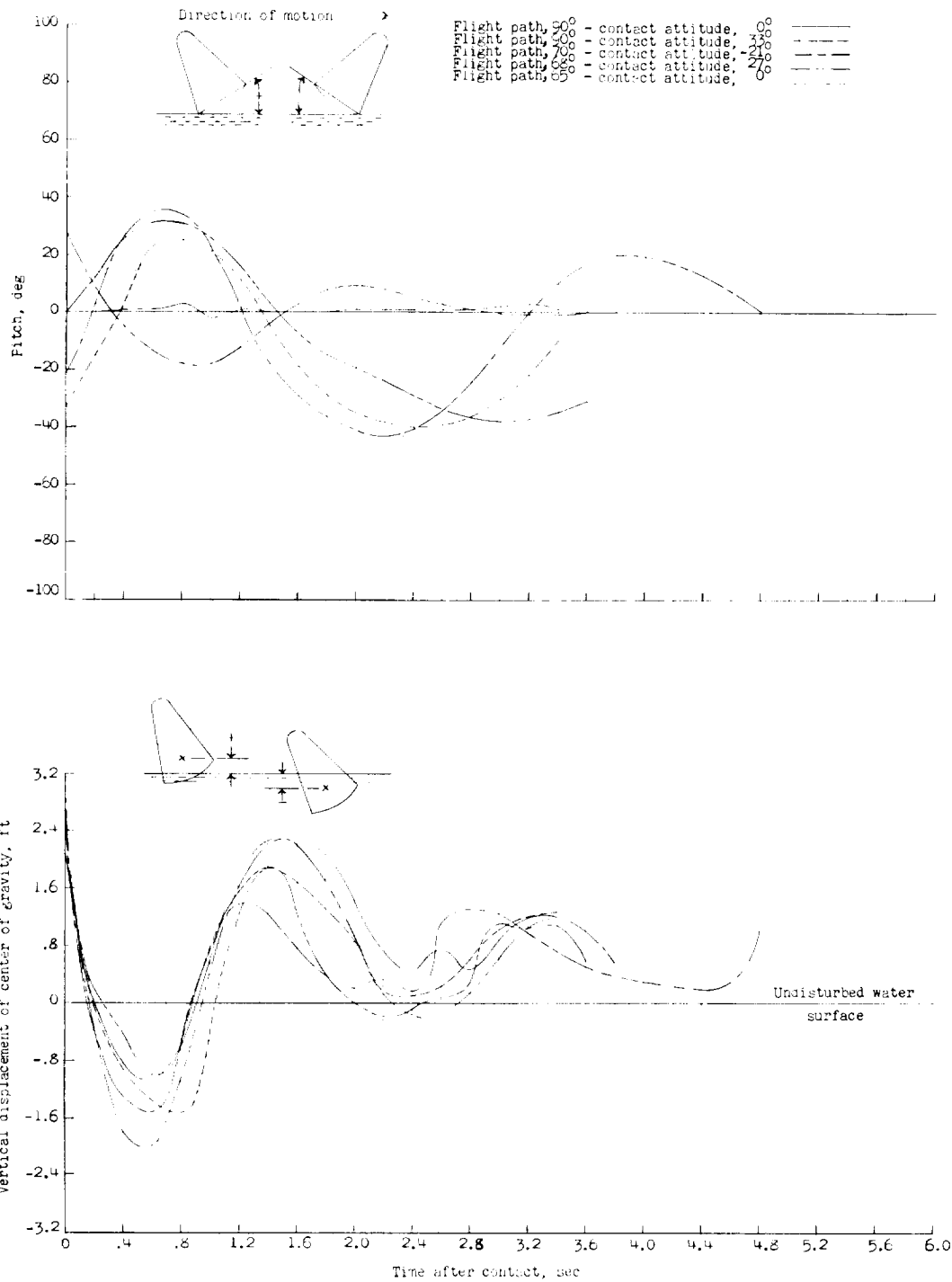


Figure 8.- Typical pitch angles and vertical displacements of the model after contact. (Values converted to full scale.)

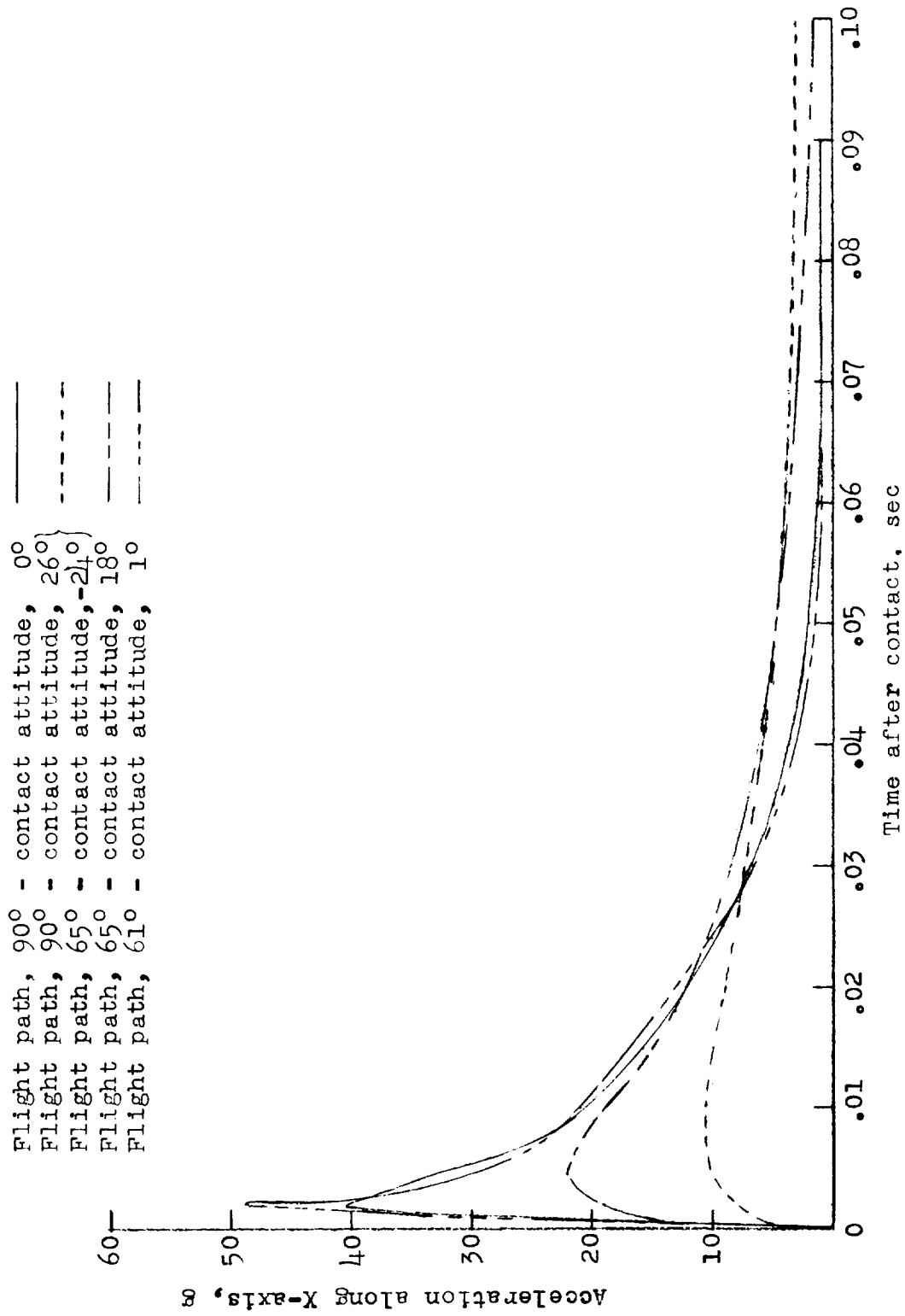
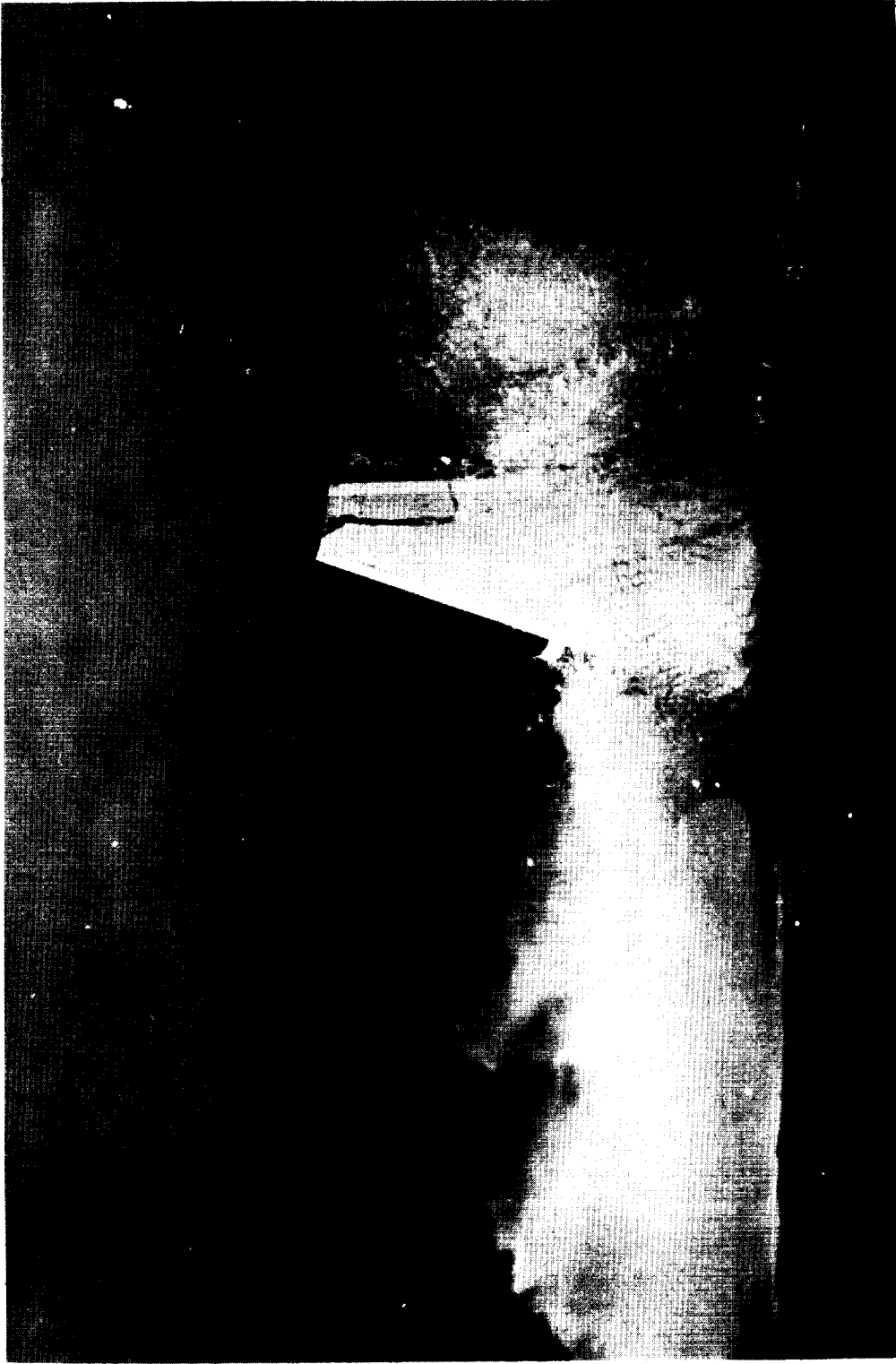


Figure 9.- Typical acceleration-time histories determined from full-scale test.





L-58-3340  
Figure 10.- Full-scale capsule after contact at an 18° attitude from a 65° flight path.

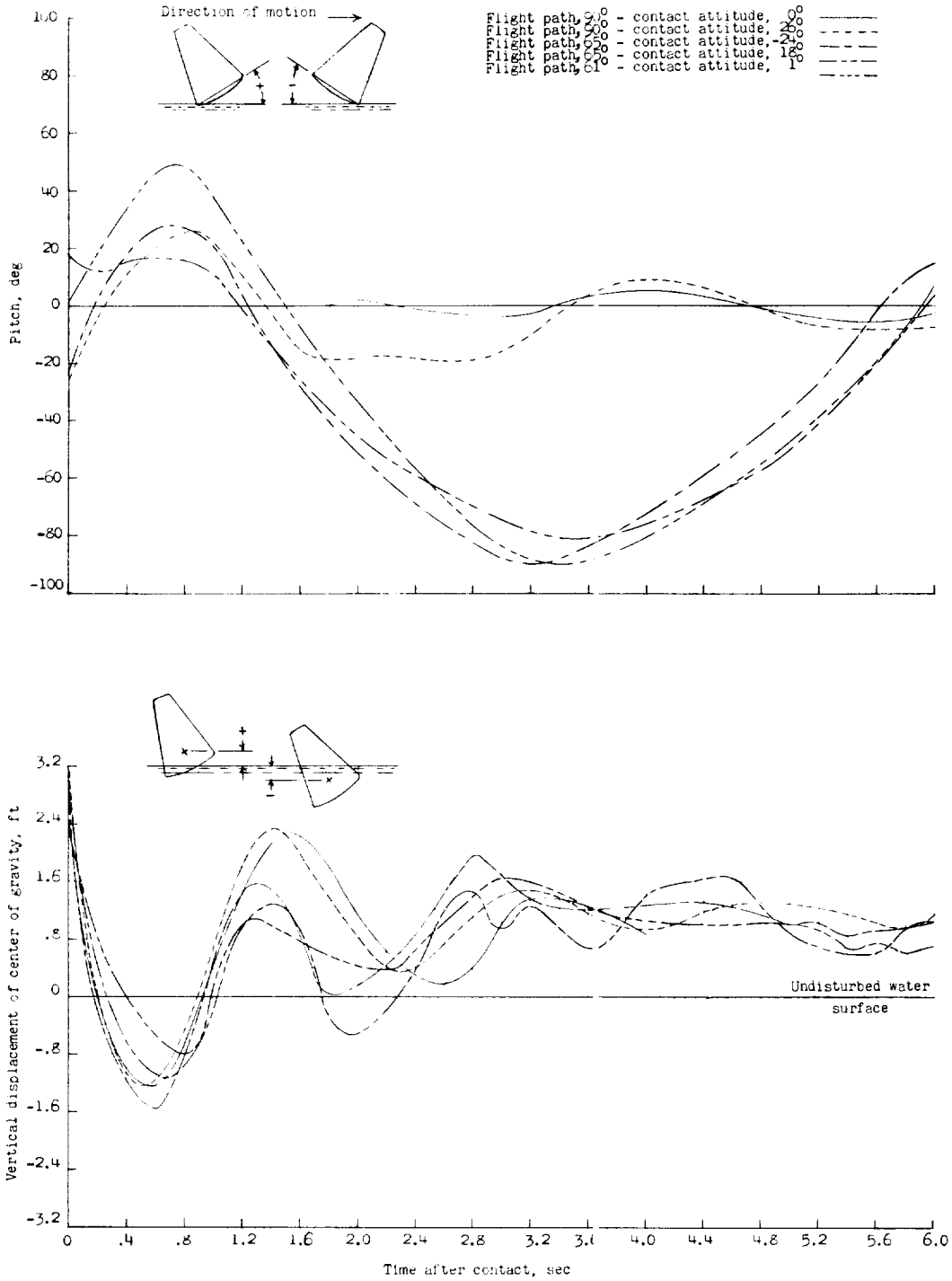


Figure 11.- Typical pitch angles and vertical displacements of full-scale capsule after contact.

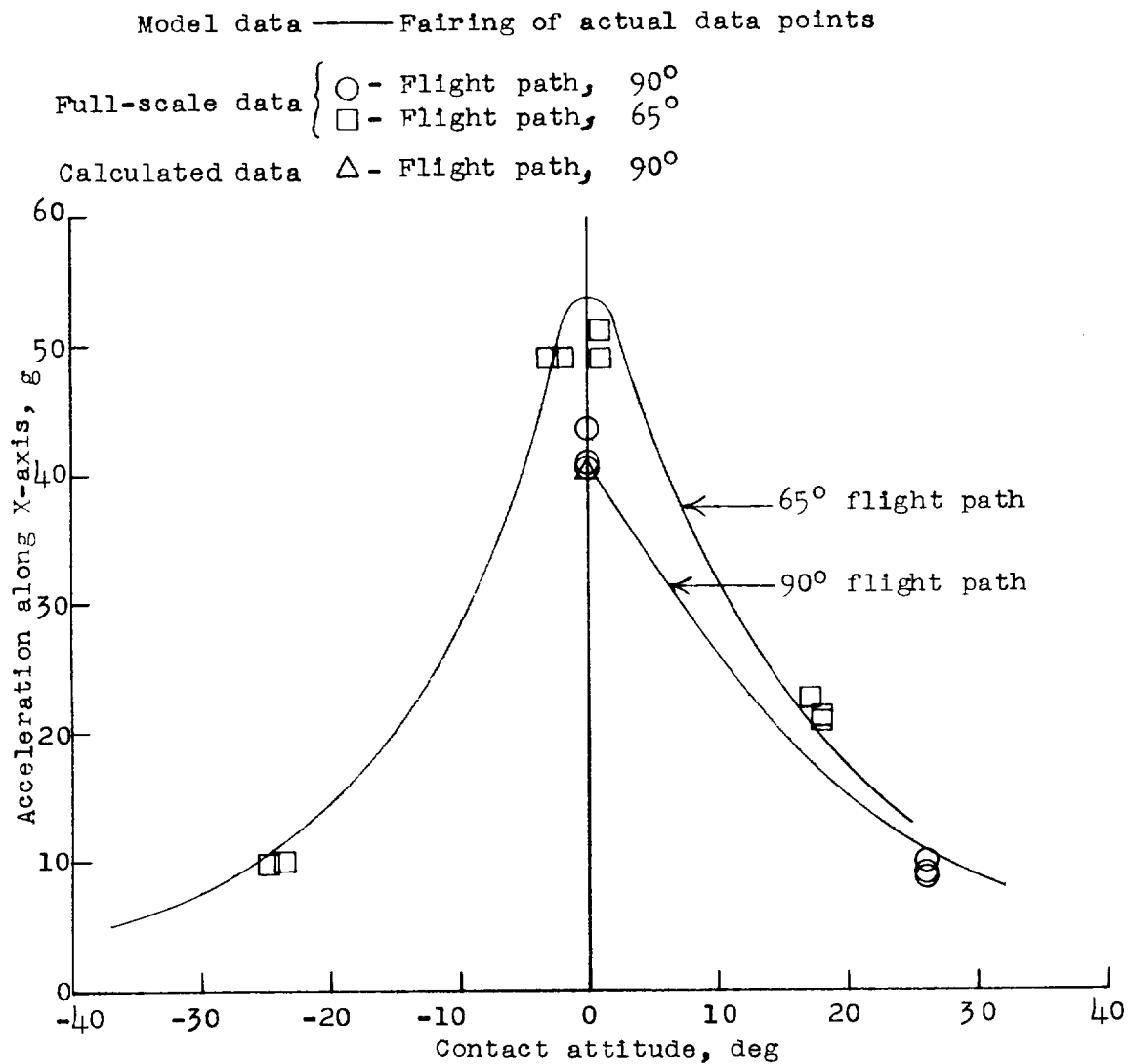


Figure 12.- Comparison of maximum accelerations along X-axis obtained from model test, full-scale test, and theoretical investigation.

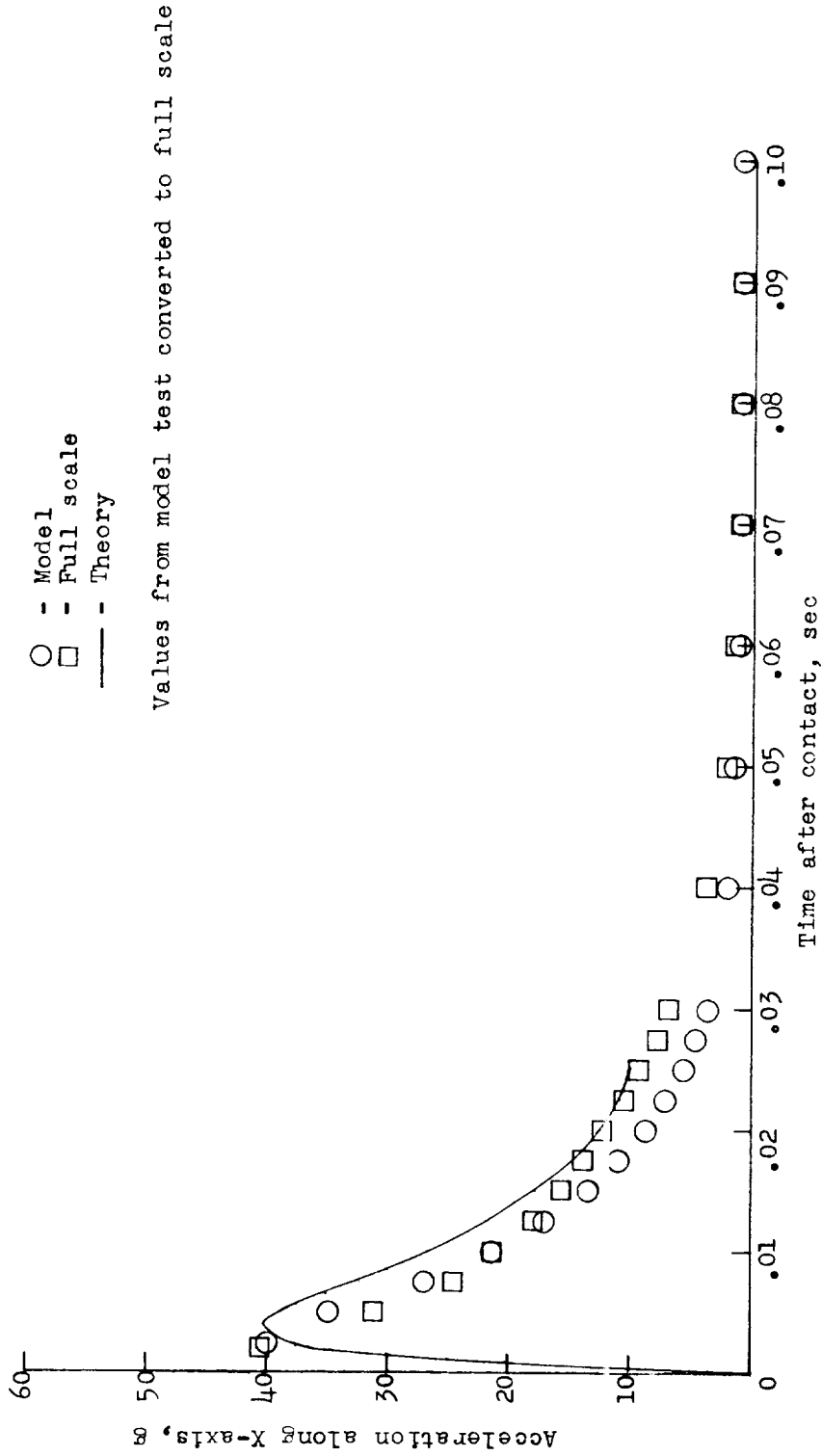


Figure 13.- Comparison of acceleration-time histories obtained from model test, full-scale test, and theoretical investigation. (Flight path, 90°; contact attitude, 0°.)